JOURNAL OF GUIDANCE, CONTROL, AND DYNAMICS
Vol. 34, No. 2, March–April 2011

Line-of-Sight Interceptor Guidance for Defending an Aircraft

Ashwini Ratnoo* and Tal Shima†
Technion–Israel Institute of Technology, 32000 Haifa, Israel

DOI: 10.2514/1.50572

A three-body interception scenario is considered, where an aircraft launches a defending missile as a counterweapon against an incoming, attacking missile. Line-of-sight guidance is investigated as a prospective strategy for the defender missile, with the aircraft being the moving launch platform. Kinematic results on line-of-sight guidance with a moving/maneuvering platform are derived, showing defender–attacker interception for all attack geometries and attacker maneuvers. The speed and maximum terminal acceleration requirements are shown to be considerably lower when compared with a proportional navigation guided defender missile. It is also shown that the attacker pays maximum penalty for an evasive maneuver from the defender if the defender uses line-of-sight guidance. A cooperative guidance law is proposed for the aircraft to maximize the attacker-to-defender lateral acceleration ratio. Simulations are carried out for various attack geometries, with and without the cooperative strategy, showing better relative control effort performance for the former.

Nomenclature

a_{me}	=	missile evasive maneuver normal to defender-missile line of sight
a_{mp}	=	missile evasive maneuver component normal to target-missile line of sight
a_t, a_d, a_m	=	target, defender, and missile lateral accelerations, respectively
$a_{t\max}$, $a_{d\max}$, $a_{m\max}$	=	target, defender, and missile maximum lateral accelerations, respectively
a_{tplos}, a_{dplos}, a_{mplos}	=	target, defender, and missile accelerations normal to the line of sight, respectively
R_d, R_m, R_{dm}	=	target-defender, target-missile, and defender-missile closing ranges, respectively
t_f	=	defender-missile interception time
v_t, v_d, v_m	=	target, defender, and missile speeds, respectively
v_{tlos}, v_{dlos}, v_{mlos}	=	target, defender, and missile speeds along the line of sight, respectively
v_{tplos}, v_{dplos}, v_{mplos}	=	target, defender, and missile speeds normal to the line of sight, respectively
γ_t, γ_d, γ_m	=	target, defender, and missile headings, respectively
λ	=	line-of-sight angle in command to line-of-sight geometry
λ_d, λ_m, λ_{dm}	=	target-defender, target-missile, and defender-missile line-of-sight angles, respectively
μ, N, η	=	target, defender, and missile navigation constants, respectively

I. Introduction

AIRCRAFT face a formidable challenge in defense against a missile attack. With missiles having considerable speed and maneuver advantages, aircraft use passive measures like flares or chaffs for evasion. In contrast, an aircraft can actively defeat the enemy missile threat by launching a countermissile in response. The resulting three-body guidance scenario is different from typical one-on-one engagements, as the aircraft can cooperate with the defender missile to intercept the attacking missile. However, it is expected that the defender missile will have no decisive speed and maneuver advantage over its adversary, and the success of the mission depends heavily on the guidance strategy used by the defending team and their cooperation.

Asher and Matuszewski [1] discussed a possible application of an optimal control-based guidance law for such a scenario. Boyell [2] presented the first results on kinematics of the three-body problem, where closed form relations were derived for constant-bearing collision courses. The ratio of launch-to-interception range was derived as a function of speed ratios. Shneydor [3], in his comments on Boyell's work [2], simplified one of the collision conditions. In a later work under the same assumptions, Boyell [4] obtained a closed-form expression for the intercept point in target-centered coordinates. Conditions for the speed ratios were also derived for different attack geometries and desired interception points. The studies with constant bearings provide valuable insight into the kinematics of the problem. However, in realistic engagements, the assumptions of constant bearings are not valid, as vehicles are expected to maneuver in order to achieve their respective objectives.

The defender missile (hereafter denoted as defender) can use proportional navigation guidance (PNG) law to keep itself on a collision course with the attacker missile (hereafter denoted as missile). Studies on classical PNG [5] law reveal that the defender should have a speed advantage over its nonmaneuvering adversary for a bounded lateral acceleration demand in all possible engagement geometries. The same requirement is increased $\sqrt{2}$ times [6,7] if the missile maneuvers while homing onto the aircraft (hereafter known as target). Absence of speed and maneuverability advantage over its adversary discourages PNG as a prospective defender guidance strategy.

Shinar and Silberman [8] solved the three-body problem as a three-player two-team game. A discrete linearized planar pursuit–evasion model was used for a preliminary investigation of the problem. The missile was assumed not to have any information about the defender, and the closing speeds were assumed to be constant. Also, the target (a ship) was assumed stationary. The study suggests that the missile should use maximum lateral acceleration for evasion near its interception by the defender. Rusnak presented a solution approach by defining the problem as a two-team dynamic game using a linearized model and a quadratic criterion [9,10]. A numerical test case was presented showing that the defender acceleration is lower than the one expected should the defender have used PNG. Recently, the three-body engagement problem received considerable attention. Perelman et al. [11] obtained an analytical solution to the linear-quadratic differential game and studied the conditions for the existence of a saddlepoint solution. Nonlinear two-dimensional simulations were used to validate the theoretical analysis. Shaferman

Received 29 April 2010; revision received 18 October 2010; accepted for publication 18 October 2010.

*Postdoctoral Fellow, Department of Aerospace Engineering; ratnoo.bkg@gmail.com.

†Senior Lecturer, Department of Aerospace Engineering; tal.shima@technion.ac.il; Associate Fellow AIAA.

and Shima [12] presented a cooperative multiple model adaptive guidance and estimation scheme applicable for the three-body problem. The filter used was a nonlinear adaptation of a multiple model adaptive estimator, in which each model represents a possible guidance law and guidance parameters of the attacking missile. It uses cooperation between the aerial target and the defender, as the defender knows the future evasive maneuvers to be performed by the protected target. Assuming no cooperation between the target aircraft and its defender missile, and that the target is nonmaneuvering, Yamasaki and Balakrishnan [13] proposed a guidance law where the defender maximizes the angle contained by its position vectors with respect to the target and the missile. Six-degree-of-freedom simulation results exemplified better defender performance, as compared with PNG.

Line-of-sight (LOS) guidance functions on the philosophy that, if an interceptor remains on the line joining the launch platform and its designated target, then it will eventually hit it. By its very nature, LOS guidance is a three-point guidance strategy. It can be implemented in two ways, namely, beam rider (BR) and command to LOS (CLOS) guidance. In BR, the missile senses its deviation from the LOS and uses this information for generating guidance commands. In CLOS implementation of the LOS guidance, the launch platform tracks both the defender and the missile. The deviation is sensed by the launch platform, and the guidance command is computed and sent to the missile through an uplink. The performance of CLOS guidance for short-range engagements is good, and the quality of the launch platform tracker limits performance in medium- to long-range applications. Studies on LOS guidance laws with a stationary launch platform are widely reported in the literature [14–17]. Kain and Yost [18] used CLOS guidance in their ship defense scenario, using Kalman filters to reduce beam jitter. Benshabat and Bar-Gill [19] proposed a robust CLOS defender guidance law for a head-on collision with a sea-skimming missile in a ship defense scenario. In their work [19], the ship was considered stationary, and the missile was assumed sea skimming in a straight line path along its LOS toward the ship.

As the main contribution of this work, we present results on kinematics of LOS guidance with a moving/maneuvering launch platform and investigate CLOS guidance as a prospective defender guidance strategy in the three-body interception scenario. Based on the kinematic results, we propose a guidance law for the defended aircraft (the launch platform) in cooperation with a CLOS guided defender in order to maximize the attacker-to-defender lateral acceleration ratio.

The remainder of the paper is arranged as follows. The three-body guidance scenario is described in Sec. II, followed by kinematic results on LOS guidance with a moving launch platform in Sec. III. Guidance laws for the defender and the target are presented in Sec. IV, and numerical simulations are presented in Sec. V. Section VI contains concluding remarks.

II. Three-Body Guidance Problem

Consider the three-body engagement scenario, as shown in Fig. 1, where the target launches a defender missile to intercept the incoming missile. We assume the three vehicles to be constant-speed point masses moving in a plane. The missile and defender are assumed to be from a similar class of vehicles, with their speeds higher than that of the target; that is,

$$v_d, v_m > v_t \tag{1}$$

The range rate and LOS rate for missile-target, defender-target, and missile-defender engagements are given as

$$\dot{R}_m = v_m \cos(\gamma_m - \lambda_m) - v_t \cos(\gamma_t - \lambda_m) \tag{2}$$

$$\dot{R}_d = v_d \cos(\gamma_d - \lambda_d) - v_t \cos(\gamma_t - \lambda_d) \tag{3}$$

$$\dot{R}_{\mathrm{dm}} = v_m \cos(\gamma_m - \lambda_{\mathrm{dm}}) - v_d \cos(\gamma_d - \lambda_{\mathrm{dm}}) \tag{4}$$

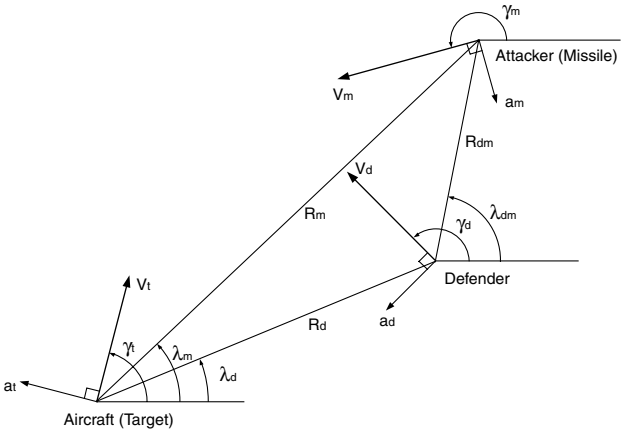

Fig. 1 Three-body engagement scenario.

and

$$\dot{\lambda}_m = \frac{v_m \sin(\gamma_m - \lambda_m) - v_t \sin(\gamma_t - \lambda_m)}{R_m} \tag{5}$$

$$\dot{\lambda}_d = \frac{v_d \sin(\gamma_d - \lambda_d) - v_t \sin(\gamma_t - \lambda_d)}{R_d} \tag{6}$$

$$\dot{\lambda}_{\mathrm{dm}} = \frac{v_m \sin(\gamma_m - \lambda_{\mathrm{dm}}) - v_d \sin(\gamma_d - \lambda_{\mathrm{dm}})}{R_{\mathrm{dm}}} \tag{7}$$

respectively. Here, γ_m, γ_t, and γ_d represent missile, target, and defender headings, respectively. And their rates are given as

$$\dot{\gamma}_m = \frac{a_m}{v_m} \tag{8}$$

$$\dot{\gamma}_d = \frac{a_d}{v_d} \tag{9}$$

$$\dot{\gamma}_t = \frac{a_t}{v_t} \tag{10}$$

where a_m, a_d, and a_t are the missile, defender, and target lateral accelerations, respectively. The acceleration capabilities for the three vehicles are limited as

$$|a_m| \le a_{m\max} \tag{11}$$

$$|a_d| \le a_{d\max} \tag{12}$$

$$|a_t| \le a_{t\max} \tag{13}$$

The three-body interception problem is an extension of the classical one-on-one interception scenario. The three vehicles have dual guidance objectives. The missile's objective is to intercept the target while successfully evading the defender. The defender has an objective of facilitating target evasion and intercepting the missile. The target has the dual objective of facilitating the missile-defender interception and successfully evading the missile. If the defender misses the missile, then the guidance problem becomes the one-on-one type, where the missile pursues and the target evades it.

III. Line-of-Sight Guidance Kinematics with a Moving/Maneuvering Launch Platform

Consider the engagement geometry, as shown in Fig. 2. We now assume that the defender follows LOS guidance, wherein it keeps its

instantaneous position on the line joining the moving launch platform (target aircraft) and the missile. This is a special case of the general three-body engagement, shown in Fig. 1, with

$$\lambda = \lambda_d = \lambda_m = \lambda_{\text{dm}} \tag{14}$$

where λ is the angle that the line joining the three vehicles makes with the reference frame. We denote this as the LOS angle. We consider the LOS course for the defender as the locus of all points between the target and the missile; that is,

$$\frac{R_d}{R_m} \in [0, 1] \tag{15}$$

At launch time, we have

$$\frac{R_d}{R_m}(0) = 0 \tag{16}$$

and at final time, we have

$$\frac{R_d}{R_m}(t_f) = 1 \tag{17}$$

where t_f is the defender-missile interception time satisfying

$$R_d(t_f) = R_m(t_f) \tag{18}$$

The velocities of the three vehicles can be expressed as the components along and normal to the LOS. Along the LOS, they are

$$v_{\text{tlos}} = v_t \cos(\gamma_t - \lambda) \tag{19}$$

$$v_{\text{dlos}} = v_d \cos(\gamma_d - \lambda) \tag{20}$$

$$v_{\text{mlos}} = v_m \cos(\gamma_m - \lambda) \tag{21}$$

and normal to the LOS, we have

$$v_{\text{tplos}} = v_t \sin(\gamma_t - \lambda) \tag{22}$$

$$v_{\text{dplos}} = v_d \sin(\gamma_d - \lambda) \tag{23}$$

$$v_{\text{mplos}} = v_m \sin(\gamma_m - \lambda) \tag{24}$$

The LOS rate of rotation can be expressed using Eqs. (14) and (22–24) in Eqs. (5) and (7), as

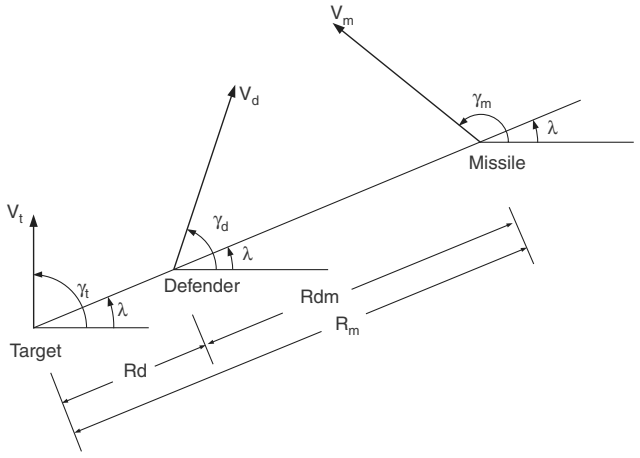

Fig. 2 LOS engagement geometry.

$$\dot{\lambda} = \frac{v_{\text{mplos}} - v_{\text{tplos}}}{R_m} = \frac{v_{\text{dplos}} - v_{\text{tplos}}}{R_d} = \frac{v_{\text{mplos}} - v_{\text{dplos}}}{R_{\text{dm}}} \tag{25}$$

And the closing speeds between the vehicles can be expressed using Eqs. (14) and (19–21) in Eqs. (2–4), as

$$\dot{R}_m = v_{\text{mlos}} - v_{\text{tlos}} \tag{26}$$

$$\dot{R}_d = v_{\text{dlos}} - v_{\text{tlos}} \tag{27}$$

$$\dot{R}_{\text{dm}} = v_{\text{mlos}} - v_{\text{dlos}} \tag{28}$$

Results on kinematics of LOS guidance with a moving/maneuvering launch platform are formally presented in the remainder of this section.

A. Speed Relations

Solving Eq. (25) for v_{dplos} and writing the velocities in time-dependent form, we have

$$v_{\text{dplos}}(t) = \frac{R_d}{R_m} v_{\text{mplos}}(t) + \left(1 - \frac{R_d}{R_m}\right) v_{\text{tplos}}(t) \tag{29}$$

At launch, we have $R_d/R_m = 0$; hence, using Eq. (29), we get

$$v_{\text{dplos}}(0) = v_{\text{tplos}}(0) \tag{30}$$

and similarly, at interception ($t = t_f$) with $R_d/R_m = 1$, we have

$$v_{\text{dplos}}(t_f) = v_{\text{mplos}}(t_f) \tag{31}$$

Equations (30) and (31) show that, during the engagement, v_{dplos} varies from a value of the target's initial speed normal to LOS to a value of missile's final speed normal to LOS. And the variation of v_{dplos} is governed by Eq. (29), where we have the required value, say $v_{\text{dplos req}}$, as

$$v_{\text{dplos req}}(t) \in [-v_m, v_m] \quad \forall\ t \in [0, t_f] \tag{32}$$

since

$$v_m > v_a, \quad \frac{R_d}{R_m} \in [0, 1]$$

Any requirement in $v_{\text{dplos req}}$ can be attained by the defender by controlling γ_d according to Eqs. (23) and (29). Considering the values of attainable v_{dplos}, say $v_{\text{dplos att}}$, we have

$$v_{\text{dplos att}}(t) = v_d \sin(\gamma_d - \lambda) \in [-v_d \quad v_d] \tag{33}$$

From Eqs. (32) and (33), we conclude that the defender can maintain the LOS course with $v_d = v_m$. Hence, with equal speed to its adversary, the defender can keep its instantaneous position on the LOS for all attack geometries and missile maneuvers.

Theorem 1: If $R_m(t_f)$ is finite, then interception between the missile and an equal speed defender is guaranteed for all attack geometries and missile maneuvers.

Proof: See Appendix.

B. Lateral Acceleration Relations

Lateral acceleration requirement is the most important characteristic of any guidance law. Next, we derive the lateral acceleration expression relating the three vehicles in the LOS geometry.

From Eq. (25), we have

$$R_m \dot{\lambda} = v_m \sin(\gamma_m - \lambda) - v_t \sin(\gamma_t - \lambda) \tag{34}$$

Differentiating Eq. (34) with respect to time yields

$$\dot{R}_m\dot{\lambda} + R_m\ddot{\lambda} = v_m\cos(\gamma_m - \lambda)(\dot{\gamma}_m - \dot{\lambda}) - v_t\cos(\gamma_t - \lambda)(\dot{\gamma}_t - \dot{\lambda}) \tag{35}$$

Using Eqs. (8) and (10) in Eq. (35), we have

$$\ddot{\lambda} = \frac{-2\dot{R}_m\dot{\lambda} + a_m\cos(\gamma_m - \lambda) - a_t\cos(\gamma_t - \lambda)}{R_m} \tag{36}$$

$$\Rightarrow \ddot{\lambda} = \frac{a_{\text{mplos}} - a_{\text{tplos}} - 2\dot{R}_m\dot{\lambda}}{R_m} \tag{37}$$

where $a_{\text{mplos}} = a_m\cos(\gamma_m - \lambda)$ and $a_{\text{tplos}} = a_t\cos(\gamma_t - \lambda)$. From Eq. (37), a_{mplos} can be derived as

$$a_{\text{mplos}} = a_{\text{tplos}} + R_m\ddot{\lambda} + 2\dot{R}_m\dot{\lambda} \tag{38}$$

A similar analysis for the defender results in

$$a_{\text{dplos}} = a_{\text{tplos}} + R_d\ddot{\lambda} + 2\dot{R}_d\dot{\lambda} \tag{39}$$

Using Eq. (38) in Eq. (39), we have

$$a_{\text{dplos}} = a_{\text{tplos}} + R_d\left(\frac{a_{\text{mplos}} - a_{\text{tplos}} - 2\dot{R}_m\dot{\lambda}}{R_m}\right) + 2\dot{R}_d\dot{\lambda} \tag{40}$$

which, on simplification, results in

$$a_{\text{dplos}} = \frac{R_d}{R_m}a_{\text{mplos}} + \left(1 - \frac{R_d}{R_m}\right)a_{\text{tplos}} + 2\dot{\lambda}\left(\dot{R}_d - \frac{R_d}{R_m}\dot{R}_m\right) \tag{41}$$

From Eq. (41), we see that the defender lateral acceleration component normal to the LOS is given as a weighted sum of target and missile lateral accelerations normal to the LOS added to a component proportional to the LOS rate. In the remainder of this section, we use this relation to derive defender lateral acceleration bounds. Also, Eq. (41) is used in Sec. IV.B to derive a cooperative guidance law for the aircraft, where it maximizes the missile-to-defender lateral acceleration.

Theorem 2: Assuming a nonmaneuvering aircraft and a missile using PNG with v_m, $v_d > 2v_t$, we obtain the following defender-to-missile acceleration relationships:

$$-1 < \frac{a_{\text{dplos}}}{a_{\text{mplos}}} < 1, \quad t \in [0, t_f] \tag{42}$$

$$-\frac{1}{3} \le \frac{a_{\text{dplos}}}{a_{\text{mplos}}} < 1, \quad t = t_f \tag{43}$$

Proof: See Appendix.

Corollary 1: If $\dot{R}_{\text{dm}}(t_f) < -v_m$, then for a LOS guided defender against a missile using PNG with a nonmaneuvering aircraft, we have

$$\frac{-1}{3} \le \frac{a_{\text{dplos}}}{a_{\text{mplos}}}(t_f) \le \frac{1}{3} \tag{44}$$

Proof: See Appendix.

Note that a defender using PNG with a navigation constant of three would require a terminal acceleration three times that of the missile [20,21]. From Theorem 2 and its Corollary, we show that LOS guidance offers much better performance in terms of terminal acceleration demand, which is critical in the present scenario with the same class of adversaries.

C. Strategy Advantage

So far, we have analyzed the three-body problem from the defender's point of view and derived results on defender speed and lateral acceleration requirements. The missile, homing on to the target, may try evading the defender, and hence would pay a penalty in terms of its maneuver requirements to hit the target aircraft. Maximizing that penalty is an important objective for the defender.

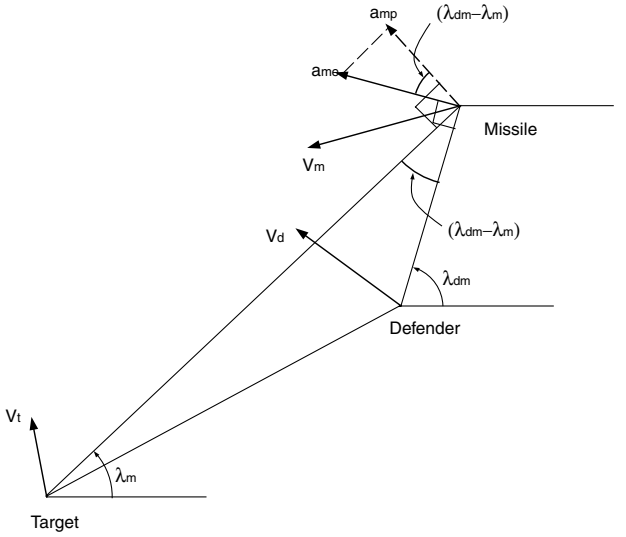

Fig. 3 Engagement scenario.

Theorem 3: The missile, on a collision course with the target, pays maximum penalty for an evasive maneuver from the defender if the defender uses LOS guidance.

Proof: We consider an engagement geometry as shown in Fig. 3, where the missile is following a collision course with the target, and the defender is pursuing the missile with a guidance strategy unknown to the missile. Sensing a closing defender, the missile performs an evasive maneuver a_{me} normal to its LOS with the defender. By performing the evasive maneuver, the missile pays a penalty, say R_p, defined as the extra distance traveled normal to its LOS with respect to the target. Let the duration of the evasive maneuver be Δt s; then, we have

$$R_p = \frac{a_{\text{mp}}}{2}\Delta t^2 \tag{45}$$

where a_{mp} is the component of a_{me} normal to its LOS with respect to the target and is expressed as

$$a_{\text{mp}} = a_{\text{me}}\cos(\lambda_{\text{dm}} - \lambda_m) \tag{46}$$

Using Eq. (46) in Eq. (45), we have

$$R_p = \frac{a_{\text{me}}}{2}\Delta t^2\cos(\lambda_{\text{dm}} - \lambda_m) \tag{47}$$

From Eq. (47), it is clear that R_p is maximum for $\lambda_{\text{dm}} = \lambda_m$, that is, if the defender uses LOS guidance. □

IV. Guidance Laws

A. Command Line-of-Sight Guidance for the Defender

The kinematics discussed in the previous section are based on ideal implementation of the LOS geometric rule; that is, the defender is always positioned on the missile-target LOS. However, in real implementation, the defender may not always be exactly on an LOS course. Consequently, Eq. (14) and the defender guidance law thus derived in Eq. (39) are no longer valid. The various reasons for the defender to not be on a perfect LOS course are as follows:

1) The estimation of guidance parameters like LOS angles, LOS separations, and their derivatives are prone to be noisy.

2) The flight control system delays are not taken into account while deriving the LOS geometric relations discussed so far. The lag needs to be compensated or, at the least, its effect has to be accounted via feedback in the guidance loop.

3) Because of practical limitations in some engagement scenarios, it is not feasible for the defender to follow the LOS course at launch.

To develop LOS geometric rule as an implementable feedback guidance law, two practical mechanizations are widely reported in the literature: namely, the BR and the CLOS. In BR, there is an electro-optical beam that joins the launch platform with the missile. The defender guidance system, which is located inside the defender, senses the deviation of the defender position from the beam and generates guidance commands to enable the defender to stay inside the beam. In CLOS guidance, an uplink is used to transmit guidance commands from a guidance computer, situated on the launch platform, to the defender. The launch platform tracks the defender and the missile, measures range, LOS angle, and LOS rate information, computes the guidance command that would enable the defender to remain on the LOS joining the launch platform and the defender, and transmits this guidance command to the defender via an uplink. Although BR is easy to implement, from an instrumentation point of view, its performance deteriorates against a maneuvering missile, since the motion of the beam is not fed forward to the defender.

The ideal defender CLOS guidance law can be written using Eq. (39), assuming $a_{\text{dplos}} = a_d$ and $a_{\text{tplos}} = a_t$, as

$$a_d = a_t + R_d\ddot{\lambda}_m + 2\dot{R}_d\dot{\lambda}_m \tag{48}$$

Note that a_d, derived in Eq. (48), comprises conventional ideal CLOS guidance acceleration terms [21] and an additional a_t term, which corresponds to the launch platform acceleration. The realistic CLOS guidance command can be obtained from the ideal command given in Eq. (48) as

$$a_d = KG(s)R_d(\lambda_m - \lambda_d) + a_t + R_d\ddot{\lambda}_m + 2\dot{R}_d\dot{\lambda}_m \tag{49}$$

where $(\lambda_m - \lambda_d)$ is the angular error between the defender LOS and the missile LOS, with

$$G(s) = \frac{1 + (s/a)}{1 + (s/b)}, \qquad b > a \tag{50}$$

being a lead network that provides the derivative control. The block diagram for CLOS guidance law is given in Fig. 4. The representation is the same as that presented by Zarchan [21], with an additional a_t term fed forward for the launch platform acceleration.

B. Cooperative Guidance Law for the Aircraft

Theorem 3 proves that the missile pays maximum penalty for an evasive maneuver from the defender if the defender follows an LOS course. However, the penalty was evaluated with a noncooperative target. Equation (41) shows that the defender's lateral acceleration demand is a function of target maneuver, missile maneuver, the LOS rate, and other kinematic parameters. An interesting aspect of the three-body engagement scenario is the cooperation between the target and the defender to achieve a common objective. The common objective here is to maximize missile lateral acceleration relative to the defender.

Let the target aircraft use a proportional navigationlike guidance law given as

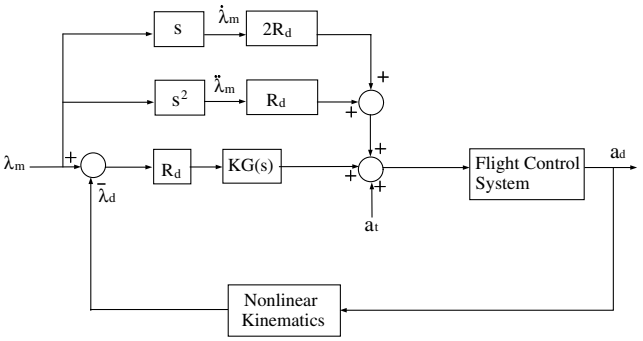

Fig. 4 Block diagram for defender CLOS implementation.

$$a_{\text{tplos}} \simeq a_t = -\mu\dot{\lambda} \tag{51}$$

where μ is positive. The negative multiplier $-\mu$ keeps the target away from a collision course with the missile, increases the absolute LOS rate, and hence induces an extra penalty on the missile. Now, the general form of the homing guidance law used by the missile can be written as

$$a_{\text{mplos}} = \eta\dot{\lambda}\cos(\gamma_m - \lambda) \tag{52}$$

($\eta > 0$ for homing)

$$\simeq -\eta\dot{\lambda} \tag{53}$$

since

$$\cos(\gamma_m - \lambda) < 0$$

Using Eqs. (41), (51), and (53), the ratio of the defender-to-missile lateral acceleration can be written as

$$\frac{a_{\text{dplos}}}{a_{\text{mplos}}} = \frac{R_d}{R_m} + \frac{\mu(1 - R_d/R_m) - 2[\dot{R}_d - (R_d/R_m)\dot{R}_m]}{\eta} \tag{54}$$

The target cooperative maneuver's objective is to 1) maximize missile lateral acceleration, and hence maximize μ; and 2) simultaneously maintain $a_{\text{dplos}}/a_{\text{mplos}} < 1$ during the engagement. Hence, we solve for the maximum value of μ such that

$$\frac{a_{\text{dplos}}}{a_{\text{mplos}}} = \frac{R_d}{R_m} + \frac{\mu(1 - R_d/R_m) - 2[\dot{R}_d - (R_d/R_m)\dot{R}_m]}{\eta} < 1 \tag{55}$$

$$\Rightarrow \mu < \frac{2[\dot{R}_d - (R_d/R_m)\dot{R}_m]}{1 - R_d/R_m} + \eta \tag{56}$$

$$\Rightarrow \mu < \frac{2\dot{R}_d}{1 - R_d/R_m} + \eta \tag{57}$$

assuming

$$\dot{R}_m < 0$$

$$\Rightarrow \mu < 2\dot{R}_d + \eta \tag{58}$$

assuming

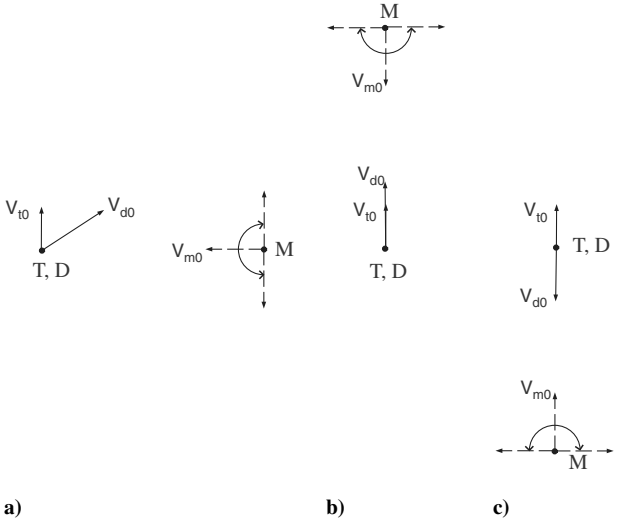

Fig. 5 Attack geometries: a) side on, b) head on, and c) tail chase.

Table 1 Engagement parameters for the three attack geometries

Parameter	Side-on geometry	Head-on geometry	Tail-chase geometry
λ_{t0}, deg	0	90	270
$R_d(0) = R_{\mathrm{dm}}(0)$, km	5	5	5
γ_{t0}, deg	90	90	90
γ_{d0}, deg	19.47	90	270
$\gamma_{m0} \in$, deg	(90, 270)	(180, 360)	(0, 180)

$$\dot{R}_d > 0$$

with

$$\frac{R_d}{R_m} \geq 0$$

Using Eq. (58) for the maximum possible value of μ, we have the target cooperative guidance law as

$$a_t = -2\dot{R}_d\dot{\lambda} \tag{59}$$

Please note that the guidance law is derived using the assumption $a_t \sim a_{\mathrm{tplos}} = a_t \cos(\gamma_t - \lambda)$. However, the signs of a_t and a_{tplos} are the same only for $-\pi/2 < \gamma_t - \lambda < \pi/2$. Hence, the cooperative law presented in Eq. (59) is modified as follows for realistic implementations:

$$a_t = \begin{cases} 2\dot{R}_d\dot{\lambda} & \text{if } -\pi/2 \geq \gamma_t - \lambda \geq \pi/2 \\ -2\dot{R}_d\dot{\lambda} & \text{if } -\pi/2 < \gamma_t - \lambda < \pi/2 \end{cases} \tag{60}$$

V. Simulations

To compare CLOS performance, with respect to PNG, and to highlight its inherent three-point guidance logic, we first carry out simulations with no aircraft cooperation. Next, simulation studies are carried out with the cooperative strategy.

A. Vehicle Models and Attack Geometries

We consider a planar engagement scenario with constant-speed point mass vehicles. The equations of motion are given as

$$\dot{x}_i = v_i \cos\gamma_i \tag{61}$$

$$\dot{y}_i = v_i \sin\gamma_i \tag{62}$$

$$\dot{\gamma}_i = \frac{a_i}{v_i} \tag{63}$$

where $i = t$, d, and m for target, defender, and missile, respectively. The speeds of the adversaries are chosen as $v_d = v_m = 600$ m/s and $v_t = 200$ m/s. The target lateral acceleration a_t for cooperative

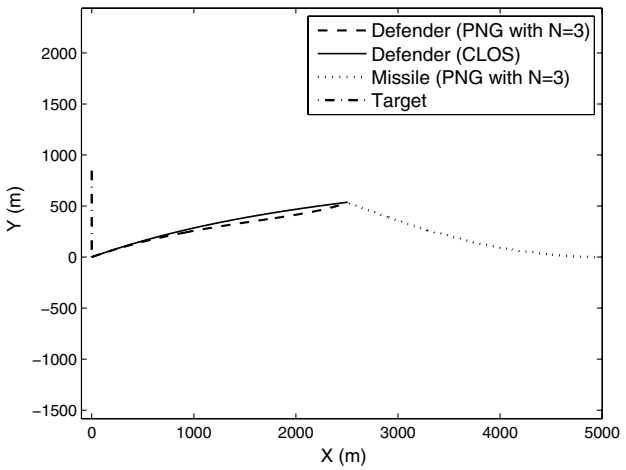

a) Trajectories

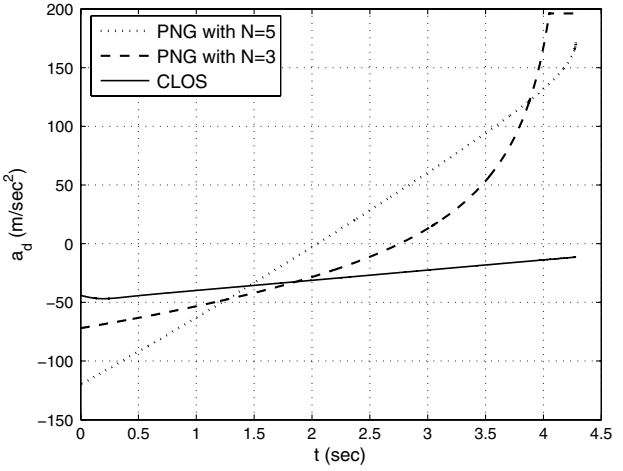

b) Defender lateral acceleration

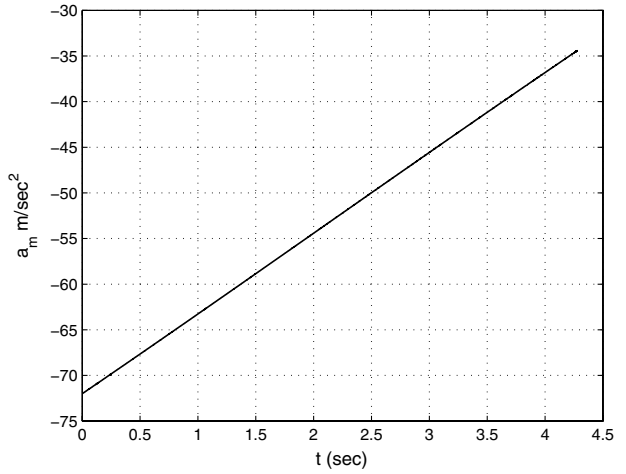

c) Missile lateral acceleration

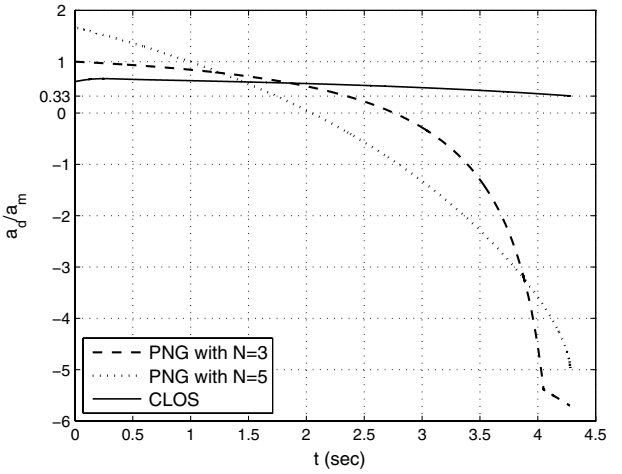

d) Defender to missile lateral acceleration ratio

Fig. 6 Side-on attack geometry: sample engagement ($\gamma_d = 19.47$ deg, and $\gamma_m = 180$ deg]).

engagements is given by Eq. (60). The defender's lateral acceleration a_d is the CLOS command given by Eq. (49) with $K = 20$, $a = 2$, and $b = 20$. The missile uses PNG with a navigation constant of three to home onto the target. The defender and the missile have a lateral acceleration capability bounded by ± 20 g, whereas the target is assumed to pull a maximum of ± 7 g. Vehicles have lag-free dynamics and use perfect information. Initial separation between the missile and the target is 5 km. Both the defender and missile are launched simultaneously at $t = 0$. We consider three standard attack geometries: namely, the side-on, the head-on, and the tail-chase engagements, as shown in Fig. 5. Here, T, D, and M represent target, defender, and missile initial positions in the plane. The classification is based on initial vehicle headings and the initial LOS angle. The engagement parameters defining the three attack geometries are listed in Table 1. We consider a missile launch envelope of 180 deg. Note that the defender launch angle for each sample engagement is chosen such that it satisfies Eq. (30) for the LOS course. The simulations are carried out using the MATLAB® ode45 solver. All simulated engagements are terminated at a defender-missile closing range of 0.1 m, unless stated otherwise.

B. Nonmaneuvering Aircraft

1. *Case 1: Side-On Attack Geometry*

Sample trajectories for a side-on engagement, with parameters as listed in Table 1, with $\gamma_{m0} = 180$ deg are plotted in Fig. 6a. The solid line shows the trajectory for the CLOS guided defender and the dashed line shows the comparative trajectory for the PNG ($N = 3$) law. The corresponding defender lateral acceleration profiles are plotted in Fig. 6b. The magnitude of CLOS lateral acceleration demand reduces with time, whereas the PNG ($N = 3$) command saturates near the missile-defender interception. The lateral acceleration demand for PNG ($N = 5$) is bounded, although it is higher than the CLOS demand. Figure 6c shows the missile lateral acceleration command, which is the typical PNG ($N = 3$) profile. The defender-to-missile lateral acceleration ratios are plotted in Fig. 6d with dashed (PNG with $N = 3$), dashed–dotted (PNG with $N = 5$), and solid lines (CLOS). The ratio is high for PNG laws and reaches a maximum absolute value greater than five near interception. On the other hand, CLOS defender lateral acceleration is always less than that of the missile; that is, $a_d/a_m < 1$ as claimed in Theorem 2. Also, the terminal value $a_d(t_f)/a_m(t_f)$ goes to 0.33, which satisfies the kinematic bound given by the Corollary to Theorem 2. To study the capturability performance of the CLOS guidance with respect to various side-on attack geometries, we vary the missile firing angle γ_{m0} and evaluate the miss distance. The capturability results for different missile firing angles and a launch range of 30 km are plotted in Fig. 7a. The miss-distance error is negligible for CLOS guidance and for PNG with $N = 5$, whereas the lateral acceleration saturation limits the capturability for PNG with $N = 3$. The total control effort $\int a_d^2\,\mathrm{d}t$ used by the defender is plotted

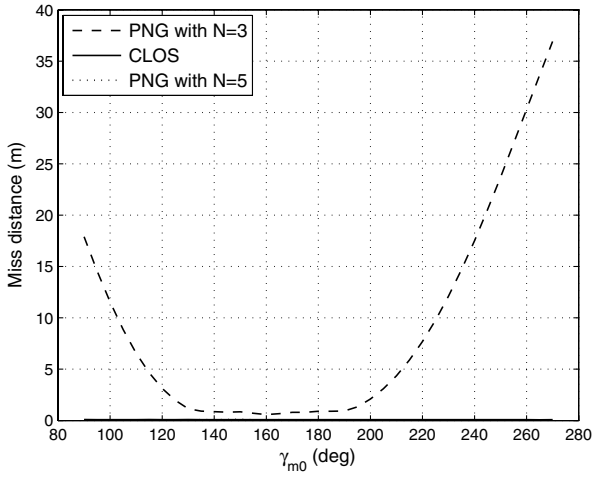

a) Miss distance vs missile firing angle

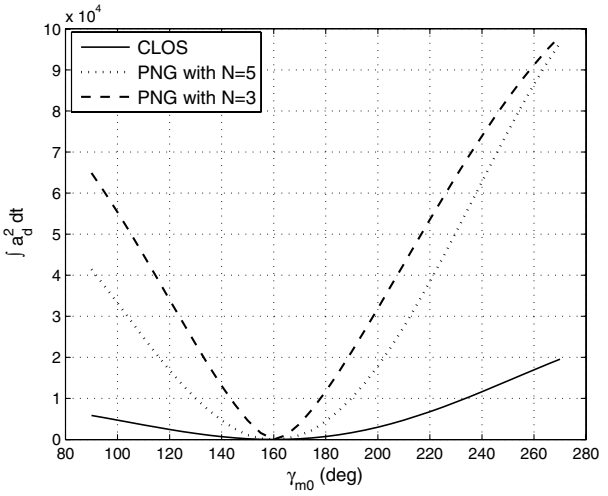

b) Total control effort vs missile firing angle

Fig. 7 Side-on attack geometry: capturability results.

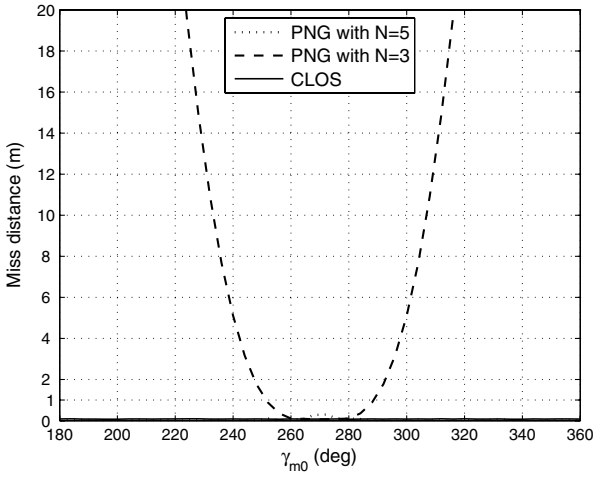

a) Miss distance vs missile firing angle

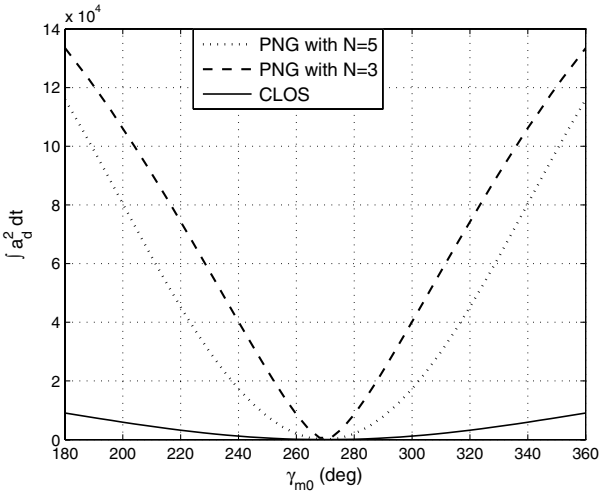

b) Total control effort vs missile firing angle

Fig. 8 Head-on attack geometry: capturability results.

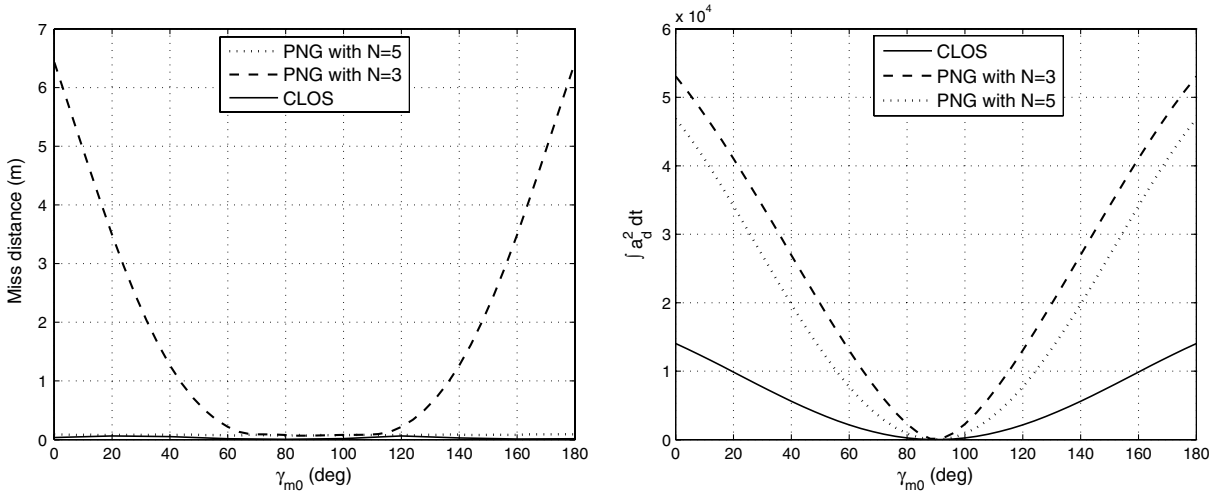

a) Miss distance vs missile firing angle **b) Total control effort vs missile firing angle**

Fig. 9 Tail-chase attack geometry: capturability results.

in Fig. 7b. CLOS guidance requires the least control effort followed by PNG ($N = 5$), with PNG ($N = 3$) requiring the highest.

2. Case 2: Head-On Attack Geometry

The miss-distance results are plotted in Fig. 8a, showing negligible errors for CLOS guidance and for PNG ($N = 5$). The capturability of PNG with $N = 3$ further deteriorates as compared to the side-on case. This is because head-on engagements close faster, causing the lateral acceleration to saturate faster. The corresponding integral control efforts are plotted in Fig. 8b. Higher lateral acceleration demand in head-on engagements causes the total control effort to also rise for the three guidance laws, with a similar relative trend as the side-on engagement scenario. The CLOS guidance law performs the best, resulting in the lowest total control effort requirement.

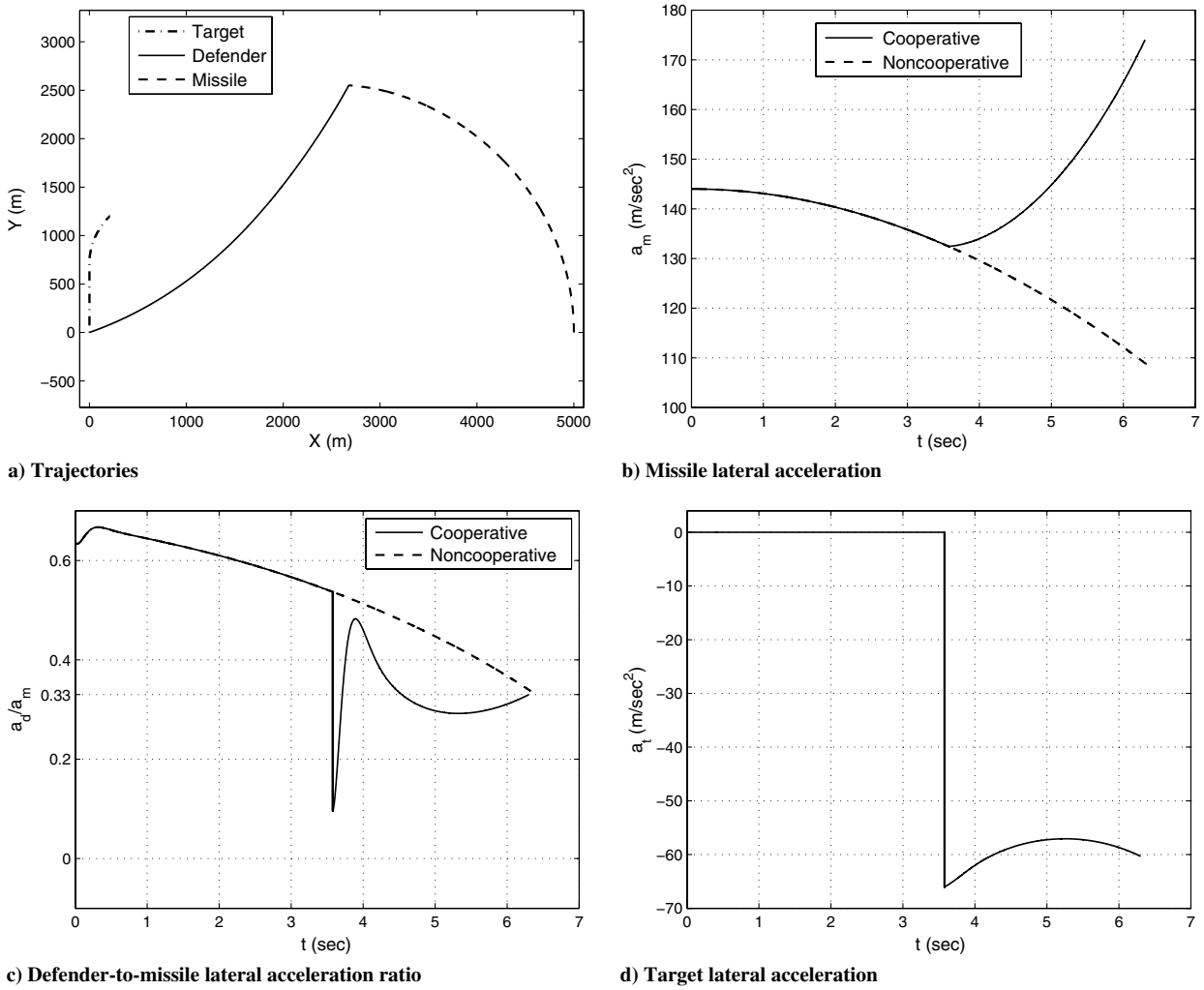

a) Trajectories **b) Missile lateral acceleration**

c) Defender-to-missile lateral acceleration ratio **d) Target lateral acceleration**

Fig. 10 Side-on attack geometry with cooperation: sample engagement ($\gamma_d = 19.47$ deg and $\gamma_m = 90$ deg).

3. Case 3: Tail-Chase Attack Geometry

The miss distances are negligible for CLOS and PNG with $N = 5$, as shown in Fig. 9a. Also, the miss distances for PNG with $N = 3$ are lower, although not negligible, as compared with the previous geometries. The control effort trends, as plotted in Fig. 9b, show the same relative trend for CLOS and PNG variants as the side-on and the head-on engagements. However, the absolute magnitudes of control efforts are lower than the side-on and the head-on cases. This can be credited to the fact that, in tail-chase attack geometries, the engagement closes at a relatively slow speed and corresponding acceleration demands are less. The CLOS guidance law again gives better performance as compared with the PNG variants.

C. Cooperative Aircraft

The target, owing to its speed disadvantage, cannot fulfil the cooperative objective of controlling the LOS rate for long. As the aircraft maneuvers away from the LOS, a_{tplos} decreases, hence reducing the aircraft's capability to control the LOS rate. Consequently, we initiate the cooperative target maneuver when the missile is at a separation of half that of the launch separation from the defender.

1. Case 4: Side-On Attack Geometry

The engagement parameters are the same as in case 1, with $\gamma_{m0} = 90$ deg. The missile, target, and defender trajectories are plotted in Fig. 10a, showing successful interception of the missile by the defender. The missile lateral acceleration is plotted in Fig. 10b with the solid line, and the corresponding lateral profile with the noncooperative strategy is shown by the dashed line. As the target-defender cooperative strategy is initiated, the missile's lateral acceleration starts increasing because of increasing LOS rate. The corresponding relative defender accelerations are plotted in Fig. 10c. The defender lateral acceleration reduces as the cooperation is initiated, and it terminates at a value of $a_d/a_m(t = t_f) = 0.33$, again conforming to Theorem 2 and its Corollary. Figure 10d shows the lateral acceleration profile for the target, which flies level until cooperation is initiated and thereafter switches to the cooperative maneuver. To evaluate the overall advantage of using the cooperative strategy, we determine the value of the relative control effort $\int a_m^2\,\mathrm{d}t / \int a_d^2\,\mathrm{d}t$ for all $\gamma_{m0} \in [90,\ 270]$ deg in the side-on geometry. The relative control effort results for cooperative and noncooperative strategies are plotted in Fig. 11 with solid and dashed lines, respectively. The results show that with cooperation, the relative control effort is higher for the missile, as compared with the case where there is no cooperation between the defender and the target. The relative control effort advantage for the cooperative strategy is high near $\gamma_{m0} = 90$ deg, and the advantage reduces until $\gamma_{m0} = 162$ deg, where the vehicles are on a collision course at the launch. The advantage is relatively lower for $\gamma_{m0} > 162$ deg, since

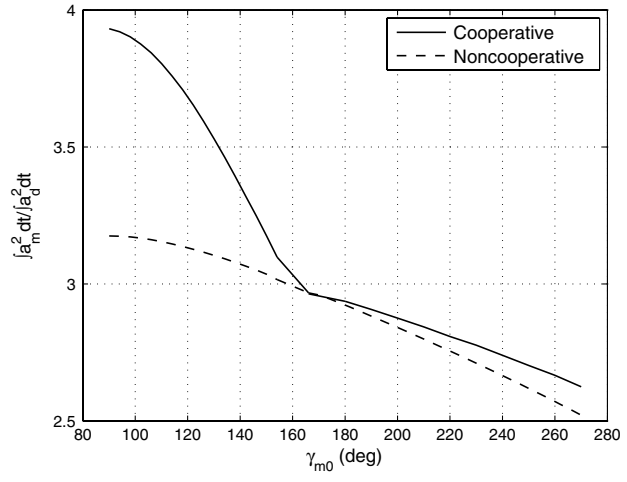

Fig. 11 Side-on attack geometry: control effort comparison.

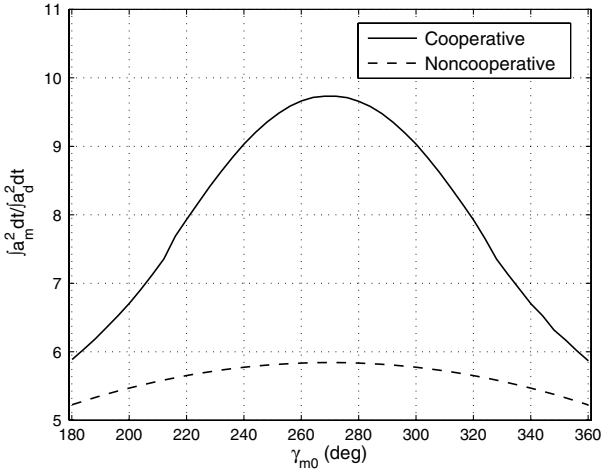

Fig. 12 Head-on attack geometry: control effort comparison.

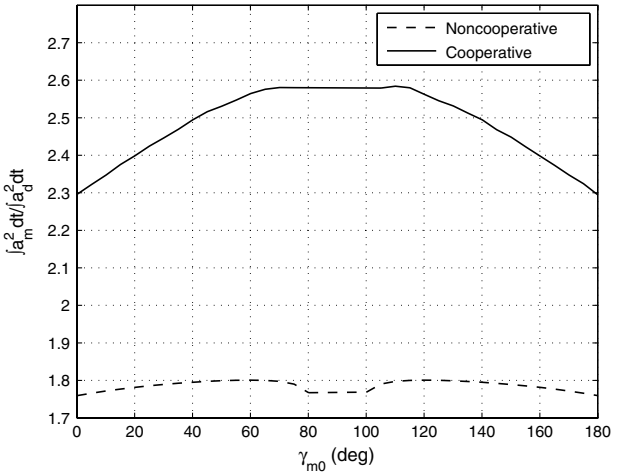

Fig. 13 Tail-chase attack geometry: control effort comparison.

$|\gamma_t - \lambda_m| > \pi/2$ for a considerable time, and the aircraft's maneuver component along the LOS is relatively smaller.

2. Case 5: Head-On Attack Geometry

We carry out the relative control effort study with cooperation for the head-on case with the engagement parameters of case 2. The results for cooperative and noncooperative strategies are plotted in Fig. 12 with solid and dashed lines, respectively. The control effort advantage is higher in the head-on case, as the engagements close faster with higher LOS rates and the aircraft cooperative maneuvers are short and more effective.

3. Case 6: Tail-Chase Attack Geometry

Similarly, we carry out the comparative study for the tail-chase case, with the engagement parameters as in case 3. The results for cooperative and noncooperative strategies are plotted in Fig. 13 with solid and dashed lines, respectively. Here again, the missile pays higher penalty relative to the defender. However, the advantage of cooperation is relatively lower as compared with the head-on case, since the LOS rates are low with longer flight times for the vehicles.

VI. Conclusions

The three-body engagement scenario where an aircraft launches a defender missile to counter an incoming missile is investigated, and a LOS guidance scheme is proposed for the defending missile. Kinematic relations of LOS guidance with a moving/maneuvering launch platform are derived, and it is shown that no speed advantage is required by the defender to intercept the missile in all scenarios.

The defender terminal lateral acceleration requirements are typically one third of that of the adversary. Capturability and control effort comparisons show high superiority of LOS guidance over proportional navigation. A cooperative guidance law is also presented for the aircraft, which increases the missile lateral acceleration relative to the defender. The missile-to-defender total control effort increases considerably when the aircraft uses the cooperative guidance law. The missile incurs the cooperation inflicted control effort penalty for all attack geometries.

Appendix: Theorem Proofs

I. Proof of Theorem 1

We classify all possible engagements in two phases.

Case 1: $v_{\text{mplos}}(t) > v_{\text{tplos}}(t)$.

Using Eq. (29) with $v_{\text{mplos}}(t) > v_{\text{tplos}}(t)$, we have

$$v_{\text{dplos}}(t) < v_{\text{mplos}}(t) \quad \forall \ \frac{R_d}{R_m} \in [0, 1) \tag{A1}$$

$$\Rightarrow v_d^2(t) - v_{\text{dplos}}^2(t) > v_m^2(t) - v_{\text{mplos}}(t)^2 \tag{A2}$$

since

$$v_d = v_m$$

$$\Rightarrow v_{\text{dlos}}^2(t) > v_{\text{mlos}}^2(t) \tag{A3}$$

For every v_{dplos}, there exist two values of v_{dlos} given as $v_{\text{dlos}} = \pm\sqrt{v_d^2 - v_{\text{dplos}}^2}$. The negative solution corresponds to the defender LOS motion toward the target and is discarded. Therefore, we have

$$v_{\text{dlos}} \geq 0 \tag{A4}$$

Using Eq. (A4) in Eq. (A3), we get

$$v_{\text{dlos}}(t) > v_{\text{mlos}}(t) \tag{A5}$$

$$\dot{R}_{md} = \dot{R}_m - \dot{R}_d = v_{\text{mlos}}(t) - v_{\text{dlos}}(t) < 0 \tag{A6}$$

Equation (A6) shows that the defender closes on the missile during this phase and $R_{md}(t_f) = 0$ is attained.

Case 2: $v_{\text{mplos}}(t) \leq v_{\text{tplos}}(t)$.

Using Eq. (29) with $v_{\text{mplos}}(t) > v_{\text{tplos}}(t)$, we have

$$v_{\text{dplos}}(t) \leq v_{\text{tplos}}(t) \tag{A7}$$

We have $\dot{R}_d > 0$ if

$$v_{\text{dlos}} > v_{\text{tlos}} \tag{A8}$$

$$\Rightarrow v_d^2 - v_{\text{dplos}}^2(t) > v_{\text{tlos}}^2(t) = v_t^2 - v_{\text{tplos}}^2(t) \tag{A9}$$

which holds, since $v_d > v_t$ and $v_{\text{dplos}}^2 \leq v_{\text{tplos}}^2$ by Eq. (A7). With $\dot{R}_d > 0$, R_d increases and can attain any finite value of $R_m(t_f)$ for interception. □

II. Proof of Theorem 2

If the missile uses PNG law against the target, then we have

$$a_{\text{mplos}} = 3v_m\dot{\lambda}\cos(\gamma_m - \lambda) \tag{A10}$$

$$\simeq -3v_m\dot{\lambda} \tag{A11}$$

since

$$\cos(\gamma_m - \lambda) < 0$$

Using Eqs. (41) and (A11) with $a_{\text{tplos}} = 0$, we have

$$\frac{a_{\text{dplos}}}{a_{\text{mplos}}} = \frac{R_d}{R_m} - \frac{2}{3}\frac{\dot{R}_d - (R_d/R_m)\dot{R}_m}{v_m} \tag{A12}$$

Differentiating Eq. (A12) partially with respect to R_d/R_m, we have

$$\frac{\partial(a_{\text{dplos}}/a_{\text{mplos}})}{\partial(R_d/R_m)} = 1 + \frac{2}{3}\frac{\dot{R}_m}{v_m} \geq 1 - \frac{2}{3}\frac{v_m + v_t}{v_m} \tag{A13}$$

since $\dot{R}_m|_{\min} = -v_m - v_t$.

Given $v_m > 2v_t$, we obtain

$$\frac{\partial(a_{\text{dplos}}/a_{\text{mplos}})}{\partial(R_d/R_m)} \geq \frac{1}{3} - \frac{2}{3}\frac{v_t}{v_m} > 0 \tag{A14}$$

Equation (A14) shows that $a_{\text{dplos}}/a_{\text{mplos}}$ increases with increasing R_d/R_m. Therefore, using Eq. (A12), at $R_d/R_m = 1$ ($t = t_f$), we have

$$\left.\frac{a_{\text{dplos}}}{a_{\text{mplos}}}\right|_{\max} = \left.\left(1 - \frac{2}{3}\frac{\dot{R}_d - \dot{R}_m}{v_m}\right)\right|_{\max} \tag{A15}$$

Near interception, the defender-missile closing speed is nonnegative; that is,

$$\dot{R}_d - \dot{R}_m > 0 \qquad (t \to t_f) \tag{A16}$$

Using Eq. (A16) in Eq. (A15), we have

$$\left.\frac{a_{\text{dplos}}}{a_{\text{mplos}}}\right|_{\max} < 1 \tag{A17}$$

Similarly, using Eq. (A12) with $(R_m/R_d)(t = 0) = 0$, we have

$$\left.\frac{a_{\text{dplos}}}{a_{\text{mplos}}}\right|_{\min} = -\frac{2}{3}\left.\frac{\dot{R}_d}{v_m}\right|_{\min} \tag{A18}$$

$$= -\frac{2}{3}\frac{(v_d + v_t)}{v_d} = -\frac{2}{3} - \frac{2}{3}\frac{v_t}{v_d} > -1 \tag{A19}$$

given

$$v_d > 2v_t$$

From Eqs. (A17) and (A19), we deduce

$$-1 < \frac{a_{\text{dplos}}}{a_{\text{mplos}}} < 1 \quad \forall \ t \in [0, t_f] \tag{A20}$$

$$a_{\text{mplos}} = 3v_m(-\dot{\lambda}) \tag{A21}$$

Using Eq. (A12) at $(R_d/R_m)(t = t_f) = 1$, we have

$$\left.\frac{a_{\text{dplos}}}{a_{\text{mplos}}}(t = t_f)\right|_{\min} = \left.\left(1 - \frac{2}{3}\frac{\dot{R}_d - \dot{R}_m}{v_m}\right)\right|_{\min} \tag{A22}$$

$$= 1 - \frac{2}{3}\frac{v_m + v_d}{v_m} = -\frac{1}{3} \tag{A23}$$

since

$$v_m \sim v_d$$

From Eqs. (A17) and (A23), we have

$$-\frac{1}{3} \leq \frac{a_{\text{dplos}}}{a_{\text{mplos}}}(t_f) < 1 \tag{A24}$$

□

III. Proof of Corollary 1

Using $\dot{R}_{\mathrm{dm}}(t_f) < -v_m$ in Eq. (A15), we get

$$\frac{a_{\mathrm{dplos}}}{a_{\mathrm{mplos}}}(t_f) \leq \frac{1}{3} \tag{A25}$$

From Eqs. (A23) and (A25), we have

$$\Rightarrow \frac{-1}{3} \leq \frac{a_{\mathrm{dplos}}}{a_{\mathrm{mplos}}}(t_f) \leq \frac{1}{3} \tag{A26}$$

□

Acknowledgment

This work was sponsored by the U.S. Air Force Office of Scientific Research, Air Force Material Command, under grant number FA8655-09-1-3051.

References

[1] Asher, R., and Matuszewski, J., "Optimal Guidance with Maneuvering Targets," *Journal of Spacecraft and Rockets*, Vol. 11, No. 3, 1974, pp. 204–206. doi:10.2514/3.62041

[2] Boyell, L. R., "Defending a Moving Target Against Missile or Torpedo Attack," *IEEE Transactions on Aerospace and Electronic Systems*, Vol. 12, No. 4, 1976, pp. 522–526. doi:10.1109/TAES.1976.308338

[3] Shneydor, N. A., "Comments on 'Defending a Moving Target Against Missile or Torpedo Attack'," *IEEE Transactions on Aerospace and Electronic Systems*, Vol. 13, No. 3, 1977, p. 321. doi:10.1109/TAES.1977.308401

[4] Boyell, R. L., "Counterweapon Aiming for Defence of a Moving Target," *IEEE Transactions on Aerospace and Electronic Systems*, Vol. 16, No. 3, 1980, pp. 402–408. doi:10.1109/TAES.1980.308911

[5] Guelman, M., "A Qualitative Study of Proportional Navigaton," *IEEE Transactions on Aerospace and Electronic Systems*, Vol. 7, No. 4, 1971, pp. 637–643. doi:10.1109/TAES.1971.310406

[6] Guelman, M., "Proportional Navigation with a Maneuvering Target," *IEEE Transactions on Aerospace and Electronic Systems*, Vol. 8, No. 3, 1972, pp. 364–371. doi:10.1109/TAES.1972.309520

[7] Guelman, M., "Missile Acceleration in Proportional Navigation," *IEEE Transactions on Aerospace and Electronic Systems*, Vol. 9, No. 3, 1973, pp. 462–463. doi:10.1109/TAES.1973.309733

[8] Shinar, J., and Silberman, G., "A Discrete Dynamic Game Modelling Anti-Missile Defense Scenarios," *Dynamics and Control*, Vol. 5, No. 1, 1995, pp. 55–67. doi:10.1007/BF01968535

[9] Rusnak, I., "Acceleration Requirements in Defense Against Missile Attack," *47th Israel Annual Conference on Aerospace Science* [CD-ROM], 2007.

[10] Rusnak, I., "Guidance Laws in Defense Against Missile Attack," *IEEE 25th Convention of Electrical and Electronics Engineers in Israel*, IEEE Publ., Piscataway, NJ, 2008, pp. 90–94.

[11] Perelman, A., Shima, T., and Rusnak, I., "Cooperative Differential Games Strategies for Active Aircraft Protection from a Homing Missile," AIAA Guidance, Navigation, and Control Conference, Toronto, ON, Canada, AIAA Paper 2010-7878, 2010.

[12] Shaferman, V., and Shima, T., "Cooperative Multiple Model Adaptive Guidance for an Aircraft Defending Missile," *Journal of Guidance, Control, and Dynamics*, Vol. 33, No. 6, 2010, pp. 1801–1813. doi:10.2514/1.49515

[13] Yamasaki, T., and Balakrishnan, S. N., "Triangle Intercept Guidance for Aerial Defense," AIAA Guidance, Navigation, and Control Conference, Toronto, ON, Canada, AIAA Paper 2010-7876, 2010.

[14] Clemow, J., *Missile Guidance*, Temple Press Unlimited, London, 1960.

[15] Siegal, J., and Lee, J. G., "Evaluation of Command to Line-of-Sight Guidance for Medium Range Missiles," Temple Press Unlimited, TR 1053-2, London, 1960.

[16] Ha, I. J., and Chong, S., "Design of a CLOS Guidance Law Via Feedback Linearization," *IEEE Transactions on Aerospace and Electronic Systems*, Vol. 28, No. 1, 1992, pp. 51–63. doi:10.1109/7.135432

[17] Lee, G. T., and Lee, J. G., "Improved Command to Line-of-Sight for Homing Guidance," *IEEE Transactions on Aerospace and Electronic Systems*, Vol. 31, No. 1, 1995, pp. 506–510. doi:10.1109/7.366337

[18] Kain, J., and Yost, D. J., "Command to Line-of-Sight Guidance a Stochastic Optimal Control Problem," AIAA Guidance and Control Conference, AIAA Paper 1976-1956, 1976.

[19] Benshabat, D. G., and Bar-Gill, A., "Robust Command to Line-of-Sight Guidance via Variable-Structure Control," *IEEE Transactions on Control Systems Technology*, Vol. 3, No. 3, 1995, pp. 356–361. doi:10.1109/87.406984

[20] Shneydor, N. A., *Missile Guidance and Pursuit*, Horwood Publ., Chichester, U.K., 1998.

[21] Zarchan, P., *Tactical and Strategic Missile Guidance*, Vol. 157, Progress in Astronautics and Aeronautics, AIAA, Washington, D. C., 1994.